ChemComm

COMMUNICATION

View Article Online
View Journal | View Issue

Cite this: *Chem. Commun.*, 2021, 57, 8019

Received 27th June 2021,
Accepted 15th July 2021

DOI: 10.1039/d1cc03422g

rsc.li/chemcomm

Detection of subtle extracellular glucose changes by artificial organelles in protocells†

Dishi Wang,[ab] Silvia Moreno,[a] Susanne Boye,[a] Brigitte Voit[ab] and Dietmar Appelhans*[a]

Feedback-controlled detection of subtle changes of extracellular biomolecules as known from cells is also needed in protocells. Artificial organelles, located in protocells, detect the small variation in pH which is triggered by different amounts of invading glucose, converted by glucose–oxidase into gluconic acid. The approach paves the way for using pH fluctuations-detecting artificial organelles in the lumen of protocells.

In recent years the re-creation of cellular biochemical processes in artificial protocells has attracted considerable attention due to its great potential in the areas of synthetic biology and bioengineering.[1,2] Inspired by the hierarchically structured architecture of eukaryotic cells, the concept of compartmentalization has been introduced into the construction of artificial protocells, generating a wide range of multi-compartmentalized structures, such as polymersome-in-polymersome,[3] liposome-in-liposome,[4] and coacervate-in-proteinosome architectures[5] and complexer systems.[6–12] Thus, intracellular chemical communication and multiple complexed processes of eukaryotic cells have been successfully reproduced in these synthetic multi-compartmentalized structures, such as the chemical communication between GOx and HRP achieved in a polymer-stabilized coacervate protocell,[8] the glucose-triggered release of insulin from synthetic artificial beta cells,[13] and GOx-mediated nitric oxide production in coacervate-based protocells.[10] The studies emphasized the importance of spatial organization, at which chemical signals can be delivered within the multienzyme network in a controlled and efficient manner.

However, less attention has been paid to the examination and evaluation of pH fluctuations of intracellular processes[14–16] where multienzymatic cascade reactions can be carried out. Actually, in biological systems such as eukaryotic cells, the local environments are very discriminating for the performance of enzymes, and physiological/neutral conditions are needed for most biochemical processes. Subtle changes in the physiological conditions (*e.g.* pH, temperature, osmotic pressure) can bring dramatic effects on organelles and cell functions, finally leading to serious diseases.[17] Similarly, for artificial protocells mediated by GOx-initiated enzymatic cascade, excess glucose attack would be counterproductive for the resided multienzyme network, as the generated overly acidic microenvironment bearing radicals (H_2O_2) would be detrimental to the structure and stability of encapsulated enzymes. Thus, there is a clear need to develop a sensitive and reliable self-reporting organelle capable of evaluating the microenvironment in a biomimetic protocell and releasing a warning signal (*e.g.* fluorescent dye) if a critical condition is approaching.

The aim of this study was to detect small alterations in extracellular glucose, mimicking subtle changes in the extracellular environment of biomimetic eukaryotic cells (BEC). Gluconic acid, resulting from the conversion of glucose by glucose oxidase (GOx), induces an undesired small pH drop from physiological pH to neutral pH or slightly lower in the lumen of BEC. Thus, a subtle glucose change (≤ 0.5 mg mL^{-1}) should be indicated by the differentiation in the intensity of fluorescein (F) dye, triggered by a pH-dependent active alkaline phosphatase (ALP),[18,19] which hydrolyses the non-fluorescent fluorescein diphosphate (FDP) in the lumen of BEC. Moreover, catalase was integrated in our concept to minimize adverse effect of reactive oxygen species (ROS), H_2O_2, on organelle functions (Fig. 1).

To achieve this goal, we present a strategy to construct BEC (Fig. 1), based on polymersomes-in-proteinosome structures (PsomesP) with semipermeable and robust outer proteinaceous membrane, prepared by encapsulating ALP-loaded polymersomes (Psomes-ALP) together with free enzymes glucose oxidase (GOx) and catalase (CAT) into proteinosomes. The proteinosomes are constructed by the assembly of BSA-PNIPAAm bio-conjugates (details in ESI†).[21] Psomes-ALP as sub-compartments should avoid a next-to-next situation of ALP with GOx, due to the undesirable

[a] *Leibniz-Institut für Polymerforschung Dresden, Hohe Straße 6, D-01069 Dresden, Germany. E-mail: applhans@ipfdd.de*
[b] *Technische Universität Dresden, D-01069 Dresden, Germany*

† Electronic supplementary information (ESI) available: Experimental descriptions, including table and figure. See DOI: 10.1039/d1cc03422g

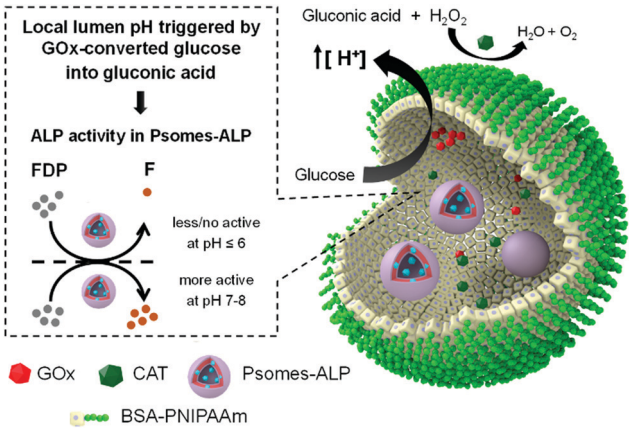

Fig. 1 3D representation of BEC based on PsomesP. Detecting subtle extracellular glucose concentration changes ($\lesssim$0.5 mg mL^{-1}), below normoglycemic conditions in blood,[20] by an enzymatic cascade reaction associated with GOx and AO, Psomes-ALP, through final detection of pH and detoxification of H_2O_2 by CAT in BEC.

production of H_2O_2 of the latter as toxic reactive oxygen species, and should, therefore, retain the enzymatic activity of ALP. Moreover, CAT is responsible for the degradation of H_2O_2. Finally, Psomes-ALP in BEC should work as adaptive and feedback-controlled artificial organelles (AO) indicating pH changes caused by the GOx-mediated oxidation of extracellular glucose within BEC, and thus being able to detect subtle changes in glucose concentration.

Our pH-responsive Psomes[22] were chosen for the establishment of AO to load ALP. Psomes-ALP were constructed and characterized, as previously reported (details in ESI†).[22–24] In this regard, the loading efficiency of ALP in Psomes was 18% (Fig. S18, S19 and Table S3, ESI†). Cryo-TEM study of Psomes-ALP confirms the expected vesicular structure (Fig. 2, ∅ 71.5 nm), as found for empty Psomes (Fig. S17, ∅ 71.3 nm, ESI†). However, the membrane thickness of Psomes-ALP is increased by ~2.7 nm compared to that of empty Psomes. The increase in membrane thickness undoubtedly results from the insertion of ALP in Psomes membrane, also described in case of avidin- and esterase-loaded Psomes.[25,26] Dynamic light scattering study further states the differences in hydrodynamic diameter between empty Psomes and purified Psomes-ALP (Table S2, ESI†).

To get a better understanding of conformation properties (*e.g.* shape and density) of Psomes-ALP, obtained by *in situ* loading, asymmetrical flow field flow fractionation in combination with light scattering detection (AF4-LS) was performed.[26] Empty Psomes were used as a reference. Firstly, the radius of gyration, R_g, is plotted *versus* the molar mass, M, (Fig. 2b and Fig. S13a, ESI†). The resulting scaling parameters of all Psomes are quite different at pH 8 and pH 6, confirming a conformation close to a hard sphere at pH 6 (parameter $\nu = 0.33$ for hard sphere). At the same time, Psomes-ALP and empty Psomes are quite similar at the same pH, indicating similar structural characteristics. Moreover, overlapping conformation characteristics of Psomes-ALP before and after HFF purification at pH 8 are indicated (Fig. 2b and Fig. S13a, b, ESI†). This fact confirms shear-force stable Psomes-ALP regarding surface and shape. Secondly, because of the interaction between Psomes membrane and ALP, ALP remains anchored in the membrane during the formation of Psomes leading to a compact, well-ordered polymeric assembly and a homogeneous membrane structure similar to empty Psomes. Nevertheless, the significant density increases for Psome-ALP at pH 8 confirms the potential location of enzymes in the Psomes lumen (Fig. 2c):[26] ρ = 0.8 (Psomes-ALP) describes a hard sphere conformation (ρ = 0.79) while 1.1 (empty Psomes) is close to a hollow sphere conformation (ρ = 1.0).[27] It implies that compared with the cavity of empty Psomes, the lumen of Psomes-ALP is additionally compacted with ALP. Same relationships can be postulated when considering AF4-LS results at pH 6 (Fig. S13e, ESI†). Interestingly, the average ρ parameters (R_g/R_h) of Psomes-ALP and Psomes increase up to 1.3 and 1.75, respectively (Fig. S13, ESI†), which can be attributed to the swelling feature of Psomes when placed at acidic condition. Overall, we can conclude that the morphology of Psomes is not changed by the *in situ* encapsulation of ALP and that ALP is located anchored at the Psomes membrane (lower apparent density (Fig. S13c and d, ESI†), but also in the lumen of Psomes (lower ρ parameter).

To develop Psomes as AO the activity of the loaded enzymes should preserve their full potential. Thus, native ALP activity has been studied compared to Psomes encapsulated ALP.

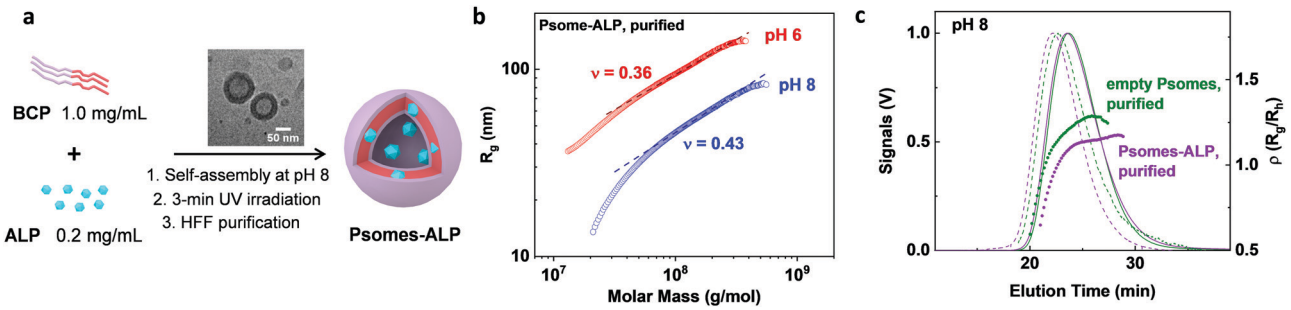

Fig. 2 Fabrication and characterisation of Psomes-ALP. General procedure for Psomes-ALP formation, with an inserted cryo-TEM image of Psomes-ALP at pH 8 (a). Dependences of radius of gyration (R_g) (b) and rho parameter (R_g/R_h) (c) on the molar mass of Psomes-ALP, compared with empty Psomes, evaluated by AF4-LS at pH 8. Determination of ρ values at highest LS signal intensity in (c).

The pH-dependent activity of native and loaded ALP was compared through an ALP assay using FDP as substrate (Fig. 1 and Fig. S15, ESI†). It shows a very steeply gradual decrease from pH 8 to 5.5 for native ALP, whereas loaded ALP exhibits a slightly higher activity. With this endowed pH-dependent profile of loaded ALP in Psomes-ALP, cyclic regulations of ALP activity with no/low activity at pH 6 and high activity at pH 8 are given (Fig. S16, ESI†). Due to the optimal activity at pH 8 and the high amount of enzyme inserted into the membrane, the activity cannot be regulated by the pH-dependent membrane permeability as previously shown.[19,20] But, Psomes offer the desired cyclic pH stability as known from previous studies (Fig. S11, ESI†).[22,23]

Finally, the pH-dependent releasing behaviour of ALP from Psomes-ALP was studied *via* a dialysis method for 24 h (details in ESI†). Surprisingly, the Psomes demonstrate an excellent ability to retain ALP in Psomes-ALP; there is no obvious release of ALP from Psomes-ALP at pH 6 or 8 (Fig. S12, ESI†).

To check whether Psomes provide a protective environment for the loaded enzymes,[23,26] the stabilization effect of Psomes was investigated by comparing the long-term activity of loaded and native ALP. At the initial stage, both of them exhibit high levels of activity. The Psomes-ALP present no loss in activity even after 10 days, while for the native ALP a gradual decay in enzyme activity can be clearly identified (Fig. S14, ESI†). This implies an improved long-term stabilizing effect for Psomes encapsulated ALP compared to native ALP.

For the development of AO in BEC (Fig. 1), Psomes-ALP undoubtedly fulfill the following required key characteristics: (i) higher enzymatic activity at neutral and basic pH than at acidic pH; (ii) pH-responsive and pH-stable; (iii) positive effect of the Psomes structures on long-term enzymatic activity of loaded ALP; and (iv) no release of ALP from Psomes-ALP at pH 6 and 8. For the adaptive and feedback-controlled AO, it is important that at acidic pH a lower enzymatic activity exists to differ between very low and low extracellular glucose concentration ($\leq$0.5 mg mL^{-1}). Firstly, AO should be sensitive at pH $\leq$ 7.4 to very low glucose concentrations $\leq$0.125 mg mL^{-1}), having at that pH an even more collapsed membrane (Fig. S21, ESI†), giving the highest ALP activity and highest fluorescence due to the FDP/F reaction. However, when the glucose concentration raises from 0.25 to 0.5 mg mL^{-1}, pH becomes more acidic due to increased GOx reaction (pH = $\leq$ 6). Here, ALP activity is reduced and, finally, switched off below pH 6, and fluorescence decreases and totally disappears. In other words, highest fluorescent detection at low glucose concentration is provided by ALP integrated in collapsed membrane of Psomes-ALP starting from physiological pH.

Using established building blocks and protocols (details and Fig. S2–S6 in ESI†) proteinosomes (P) from BSA-PNIPAAm bio-conjugates (Fig. S9, ESI†)[21] and (Psomes-ALP/GOx/CAT) in proteinosomes (PsomesP) (details in ESI†) have been constructed *via* Pickering emulsion method. The structural characterization of P and PsomesP was carried out by confocal laser scanning microscopy (CLSM), light microscopy and transmission electronic microscopy (TEM). The spherical structure of P is identified by CLSM image, and it retains a collapsed but structurally intact structure after drying in air (Fig. S7, ESI†). The molecular weight cut-off of P membrane (Fig. 1) is between 40 and 70 kDa (Fig. S8, ESI†). Thus, the required diffusion of small molecules (*e.g.* glucose) is possible, while biomacromolecules larger than 40 kDa, such as GOx, CAT and Psomes-ALP can be locked in P.

Structural composition of PsomesP is confirmed by CLSM study, using Cy5-labelled ALP in Psomes-ALP, Atto425-labelled GOx, and RhB-labelled BSA–PNIPAAm bio-conjugates (Fig. 3a–d). Considering the uniform green and blue fluorescence throughout the interior of PsomesP, the loaded GOx and Psomes-ALP are homogenously distributed in the lumen of PsomesP, while most of RhB-labelled BSA-PNIPAAm bio-conjugates are assembled into the outer membrane of PsomesP. In addition, TEM study also confirms that Psomes can retain their intact structure in P (Fig. S10, ESI†). The TEM results are similar as found in a recently published study.[6] Thus, Psomes and their resulting AO can be smoothly integrated in P, similar as observed in other approaches for the construction of BEC.[6,8]

To realize the potential of BEC for mimicking the natural communication within a cell and their response on invading small amount of glucose from the extracellular environment, the interplay between GOx, Psome-ALP and CAT was studied. The acidification of BEC lumen as response to GOx-converted glucose was validated (Fig. 1). Due to the pH responsiveness of ALP in Psomes-ALP in FDP assay (Fig. 4a), different levels of the ALP activity in the dephosphorylation of FDP into F result in a time-dependent change in fluorescence (Fig. 4c), corresponding to a time-dependent change in the pH outside and inside of BEC (Fig. 4b). After the addition of glucose (0.5 mg mL^{-1}), the acidification through GOx-converted glucose (Fig. 4b) is clearly detectable, and it leads to a fast pH drop, leveling off at approximately pH 4.0. By changing the stepwise glucose concentration from 0.5 mg mL^{-1} to 0.0 mg mL^{-1} (lower limit of detection = 0.0625 mg mL^{-1}, Fig. S23, ESI†), the rate of pH drop decreases in a gradual manner and ends at higher pH points (*e.g.* at pH 7.2 for 0.0625 mg mL^{-1}). Due to the pH responsiveness nature of ALP,[18,19] the activity of loaded ALP follows the postulated working principle of Psomes-ALP as AO (Fig. 4c). Thus, it smoothly reflects the correlation of very low glucose concentration with high ALP activity. This indicates a low production of protons which results in pH range from 7.2 to 6.8. The opposite behaviour is visible at glucose concentration of $\geq$0.25 mg mL^{-1}, but still below normoglycemic conditions in blood:[20] no/very low activity of ALP is

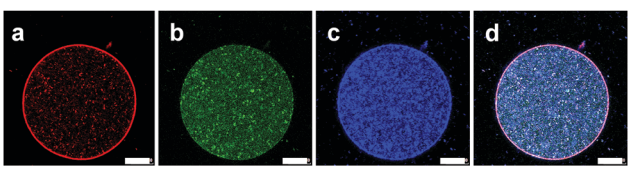

Fig. 3 Visualization of a PsomesP. Confocal fluorescence microscopy images of RhB-labelled proteinosomes (a), Psomes encapsulating Cy5-labelled ALP (b), and Atto425-labelled GOx (c) in aqueous solution. Merged image (d) shows colocalization of BSA-PNIPAAm, Psome-ALP, and GOx. Scale bar: 10 μm.

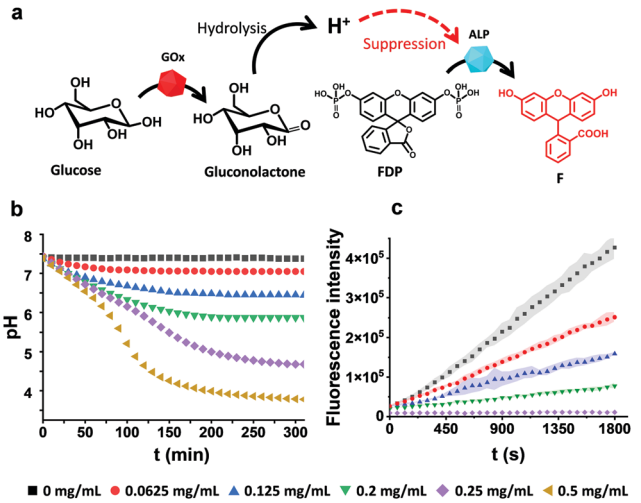

Fig. 4 Study of enzymatic cascade in PsomesP. Representation of a two-enzyme cascade reaction based on GOx and ALP; pH measured for the complete system, but also represents the local pH within BEC (a). Influence of the glucose concentration on the pH changes of the PsomesP (b). Time profile for PsomesP showing changes in fluorescence intensity of hydrolysed FDP in the presence of various glucose concentrations after 30 min. Each measurement was carried out for 3 times at least. Data are presented as mean values ± SD, error bars indicate standard deviations (n = 3) (c).

detected meaning pH $\leq$ 6 is achieved. Thus, Psomes-ALP as AO are suited to differentiate very reproducibly subtle changes in amounts of invading glucose, converted by GOx into gluconic acid; also showing a negligible variation in fluorescence for each glucose concentration. Resulting proton production orchestrate highly reproducible feedback-controlled actions of AO in BEC (Fig. 4c and Fig. S21, ESI†) that also works with simultaneous actions of GOx and Psomes-ALP in a time-dependent and feedback-controlled manner (Fig. S20 in ESI†).

In conclusion, we demonstrated a facile method for the construction of BEC where Psomes-ALP and free enzymes, GOx and CAT, can be subsequently integrated in proteinosome (PsomesP) *via* the Pickering emulsion method. The hierarchically organized compartments provide a strategy for the spatial organization of sequential and parallel enzymatic reactions, whereby functional biomacromolecules can be separated into different discrete regions without interference. Psomes-ALP employed as artificial organelles (AO) can retain their structural and functional integrity in BEC, where AO offers a protective, stabilizing and gating environment for ALP Thus, Psomes-ALP enzyme can be used as multifunctional biological unit for the detection of changes in pH in BEC.

Finally, this work provides a new approach into the detection of subtle concentration changes of extracellular nutrients and bioactive (macro)molecules, successfully exemplified by the detection of pH changes in BEC, represented by our PsomesP, through GOx-converted glucose. This paves the way to BEC mimicking intracellular homeostasis and intra-/intercellular chemical communications.

The authors gratefully acknowledge that the study was done within the Dresden International Graduate School for Biomedicine and Bioengineering (DIGS-BB). Authors thank for the discussion of this topic with Dr D. Tang, Prof. A. Lederer, and Prof. A. Temme, but also Dr P. Formanek for carrying out (cryo-)TEM study.

Conflicts of interest

There are no conflicts to declare.

Notes and references

1 Z. Liu, X. Xu and R. Tang, *Adv. Funct. Mater.*, 2016, **26**, 1862–1880.
2 S. Serrano-Luginbühl, K. Ruiz-Mirazo, R. Ostaszewski, F. Gallou and P. Walde, *Nat. Rev. Chem.*, 2018, **2**, 306–327.
3 R. J. Peters, M. Marguet, S. Marais, M. W. Fraaije, J. C. Van Hest and S. Lecommandoux, *Angew. Chem., Int. Ed.*, 2014, **126**, 150–154.
4 C. M. Paleos, D. Tsiourvas, Z. Sideratou and A. Pantos, *J. Controlled Release*, 2013, **170**, 141–152.
5 R. Booth, Y. Qiao, M. Li and S. Mann, *Angew. Chem., Int. Ed.*, 2019, **131**, 9218–9222.
6 P. Wen, X. Wang, S. Moreno, S. Boye, D. Voigt, B. Voit, X. Huang and D. Appelhans, *Small*, 2021, **17**, 2005749.
7 L. Rodríguez-Arco, B. P. Kumar, M. Li, A. J. Patil and S. Mann, *Angew. Chem., Int. Ed.*, 2019, **131**, 6399–6403.
8 A. F. Mason, N. A. Yewdall, P. L. Welzen, J. Shao, M. van Stevendaal, J. C. van Hest, D. S. Williams and L. K. Abdelmohsen, *ACS Cent. Sci.*, 2019, **5**, 1360–1365.
9 S. Deshpande, F. Brandenburg, A. Lau, M. G. Last, W. K. Spoelstra, L. Reese, S. Wunnava, M. Dogterom and C. Dekker, *Nat. Commun.*, 2019, **10**, 1–11.
10 S. Liu, Y. Zhang, M. Li, L. Xiong, Z. Zhang, X. Yang, X. He, K. Wang, J. Liu and S. Mann, *Nat. Chem.*, 2020, **12**, 1165–1173.
11 S. Thamboo, A. Najer, A. Belluati, C. von Planta, D. Wu, I. Craciun, W. Meier and C. G. Palivan, *Adv. Funct. Mater.*, 2019, **29**, 1904267.
12 A. Belluati, S. Thamboo, A. Najer, V. Maffeis, C. von Planta, I. Craciun, C. G. Palivan and W. Meier, *Adv. Funct. Mater.*, 2020, 2002949.
13 Z. Chen, J. Wang, W. Sun, E. Archibong, A. R. Kahkoska, X. Zhang, Y. Lu, F. S. Ligler, J. B. Buse and Z. Gu, *Nat. Chem. Biol.*, 2018, **14**, 86.
14 C. Love, J. Steinkühler, D. T. Gonzales, N. Yandrapalli, T. Robinson, R. Dimova and T. Y. D. Tang, *Angew. Chem., Int. Ed.*, 2020, **132**, 6006–6013.
15 R. Martí-Centelles, J. Rubio-Magnieto and B. Escuder, *Chem. Commun.*, 2020, **56**, 14487–14490.
16 N. G. Moreau, N. Martin, P. Gobbo, T.-Y. D. Tang and S. Mann, *Chem. Commun.*, 2020, **56**, 12717–12720.
17 L. Wang, J. Cao, D. Chen, X. Liu, H. Lu and Z. Liu, *Biol. Trace Elem. Res.*, 2009, **127**, 53.
18 A. Bhatti, A. Alvi, S. Walia and G. Chaudhry, *Curr. Microbiol.*, 2002, **45**, 245–249.
19 H. Zhang, L. Yang, W. Ding and Y. Ma, *J. Biol. Inorg. Chem.*, 2018, **23**, 277–284.
20 D. H.-C. Chou, M. J. Webber, B. C. Tang, A. B. Lin, L. S. Thapa, D. Deng, J. V. Truong, A. B. Cortinas, R. Langer and D. G. Anderson, *Proc. Natl. Acad. Sci. U. S. A.*, 2015, **112**, 2401–2406.
21 X. Huang, M. Li, D. C. Green, D. S. Williams, A. J. Patil and S. Mann, *Nat. Commun.*, 2013, **4**, 1–9.
22 J. Gaitzsch, D. Appelhans, L. Wang, G. Battaglia and B. Voit, *Angew. Chem., Int. Ed.*, 2012, **51**, 4448–4451.
23 D. Gräfe, J. Gaitzsch, D. Appelhans and B. Voit, *Nanoscale*, 2014, **6**, 10752–10761.
24 S. Moreno, P. Sharan, J. Engelke, H. Gumz, S. Boye, U. Oertel, P. Wang, S. Banerjee, R. Klajn, B. Voit, A. Lederer and D. Appelhans, *Small*, 2020, **16**, 2002135.
25 S. Moreno, S. Boye, A. Lederer, A. Falanga, S. Galdiero, S. Lecommandoux, B. Voit and D. Appelhans, *Biomacromolecules*, 2020, **21**, 5162–5172.
26 H. Gumz, S. Boye, B. Iyisan, V. Krönert, P. Formanek, B. Voit, A. Lederer and D. Appelhans, *Adv. Sci.*, 2019, **6**, 1801299.
27 W. Burchard, *Branched polymers II*, Springer, 1999, pp. 113–194.